Transmission of Multidrug-Resistant *Salmonella enterica* Subspecies *enterica* 4,[5],12:i:- Sequence Type 34 between Europe and the United States

Ehud Elnekave, Samuel L. Hong, Seunghyun Lim, Dave Boxrud, Albert Rovira,
Alison E. Mather, Andres Perez, Julio Alvarez

Multidrug-resistant *Salmonella enterica* subspecies *enterica* 4,[5],12:i:- sequence type 34 represents a worldwide public health risk. To determine its origin in the United States, we reconstructed a time-scaled phylogeny with a discrete trait geospatial model. The clone in the United States was introduced from Europe on multiple occasions in the early 2000s.

Since the late 1990s, reports of an emerging multidrug-resistant *Salmonella enterica* subspecies *enterica* serotype 4,[5],12:i:- strain have been published in Europe (*1*). This strain is a monophasic variant of *Salmonella* Typhimurium, predominantly resistant to ampicillin, streptomycin, sulfonamides, and tetracycline (ASSuT). Its rapid increase in North America after 1998 has also been described (*2*). However, precise knowledge of the time of introduction and the initial influx of clinical cases caused by this serotype in the United States is not available because of inconsistent reporting before 2004 (*3*).

Previously, on the basis of high genetic similarity between *Salmonella* 4,[5],12:i:- sequence type (ST) 34 isolates from the United States and Europe and *Salmonella* Typhimurium strains from Europe, we suggested a European origin for the *Salmonella* 4,[5],12:i:- ST34 clade (*4*). With this study, we aimed to reconstruct a time-scaled phylogeny of the emerging ST34 clade by using a Bayesian modeling approach to determine its origin in United States.

The Study

We used publicly available whole-genome sequences of 1,431 *Salmonella* 4,[5],12:i:- ST34 isolates from the United States and Europe from 2008–2017, including sequences from 690 isolates from Europe (mainly from the United Kingdom and Denmark) and 741 isolates from multiple US states (Appendix 1, https://wwwnc.cdc.gov/EID/article/26/12/20-0336-App1.xlsx). We used BEAST version 1.8.4 (*5*) to estimate divergence times, mutation rates, and location trait transitions. We applied the modeling approach to 10 subsets of 112 sequences selected from the study population. These sequences represented 33% (474/1,431) of the study population and included 242 sequences from Europe (76% from humans, 8% from food products, 8% from livestock, and 8% from other sources) and 232 from the United States (62% from humans, 13% from food products, 21% from livestock, and 3% from other sources). Time-scaled phylogenies of each subset were reconstructed by using a general time-reversible nucleotide substitution model, an uncorrelated lognormal relaxed molecular clock, and an exponential growth coalescent model with asymmetric trait transitions (Figure 1; Appendix 2 Figures 1–10, https://wwwnc.cdc.gov/EID/article/26/12/20-0336-App2.pdf). All time-scaled phylogenies presented similar topology to a maximum-likelihood phylogeny constructed by using all 1,431 study isolates (based on visual inspection; Appendix 2 Figure 11). Overall, averaged estimates from all subsets were in agreement as follows (Figure 2): the evolutionary rate was 3.64×10^{-7} substitutions/site/year (95% highest posterior density [HPD] $2.65–4.64 \times 10^{-7}$), which corresponds to an accumulation of ≈1–2 single-nucleotide

Author affiliations: Hebrew University of Jerusalem, Jerusalem, Israel (E. Elnekave); University of Minnesota, St. Paul, Minnesota, USA (E. Elnekave, S. Lim, A. Rovira, A. Perez, J. Alvarez); University of Leuven, Leuven, Belgium (S.L. Hong); Minnesota Department of Health, St. Paul (D. Boxrud); Quadram Institute Bioscience, Norwich, UK (A.E. Mather); University of East Anglia, Norwich (A.E. Mather); Universidad Complutense, Madrid, Spain (J. Alvarez)

DOI: https://doi.org/10.3201/eid2612.200336

polymorphisms/genome/year; the time to most recent common ancestor was 1994 (95% HPD 1988–2000); the number of collection location state transitions (Markov jumps) from Europe to the United States was 7.7 (95% HPD 5.9–9.3) and from the United States to Europe was 0.8 (95% HPD 0–2.2); and the waiting times (in years; Markov rewards) were 519.9 (95% HPD 393.1–667.8) in Europe and 318.6 (95% HPD 234.0–417.6) in the United

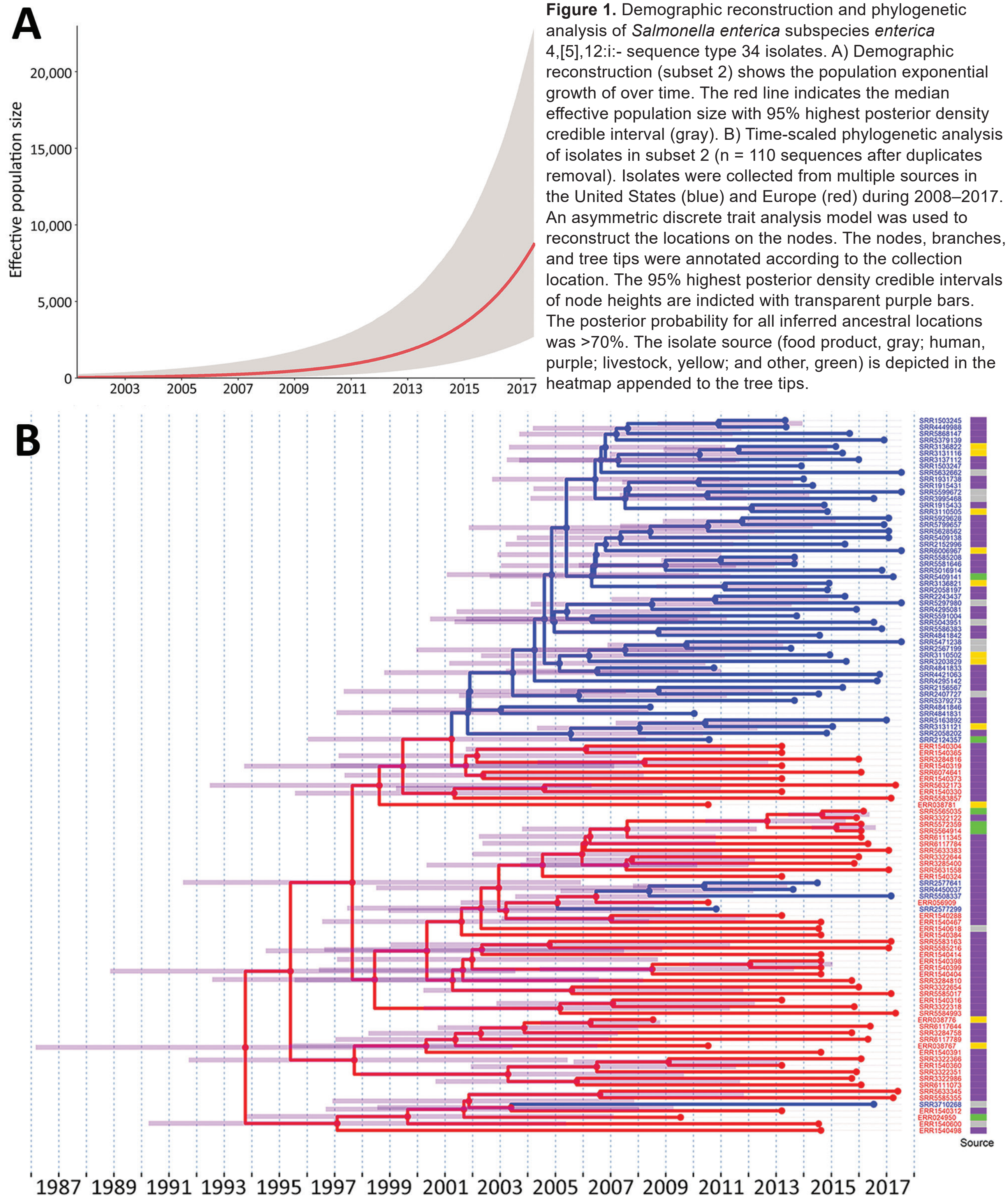

Figure 1. Demographic reconstruction and phylogenetic analysis of *Salmonella enterica* subspecies *enterica* 4,[5],12:i:- sequence type 34 isolates. A) Demographic reconstruction (subset 2) shows the population exponential growth of over time. The red line indicates the median effective population size with 95% highest posterior density credible interval (gray). B) Time-scaled phylogenetic analysis of isolates in subset 2 (n = 110 sequences after duplicates removal). Isolates were collected from multiple sources in the United States (blue) and Europe (red) during 2008–2017. An asymmetric discrete trait analysis model was used to reconstruct the locations on the nodes. The nodes, branches, and tree tips were annotated according to the collection location. The 95% highest posterior density credible intervals of node heights are indicted with transparent purple bars. The posterior probability for all inferred ancestral locations was >70%. The isolate source (food product, gray; human, purple; livestock, yellow; and other, green) is depicted in the heatmap appended to the tree tips.

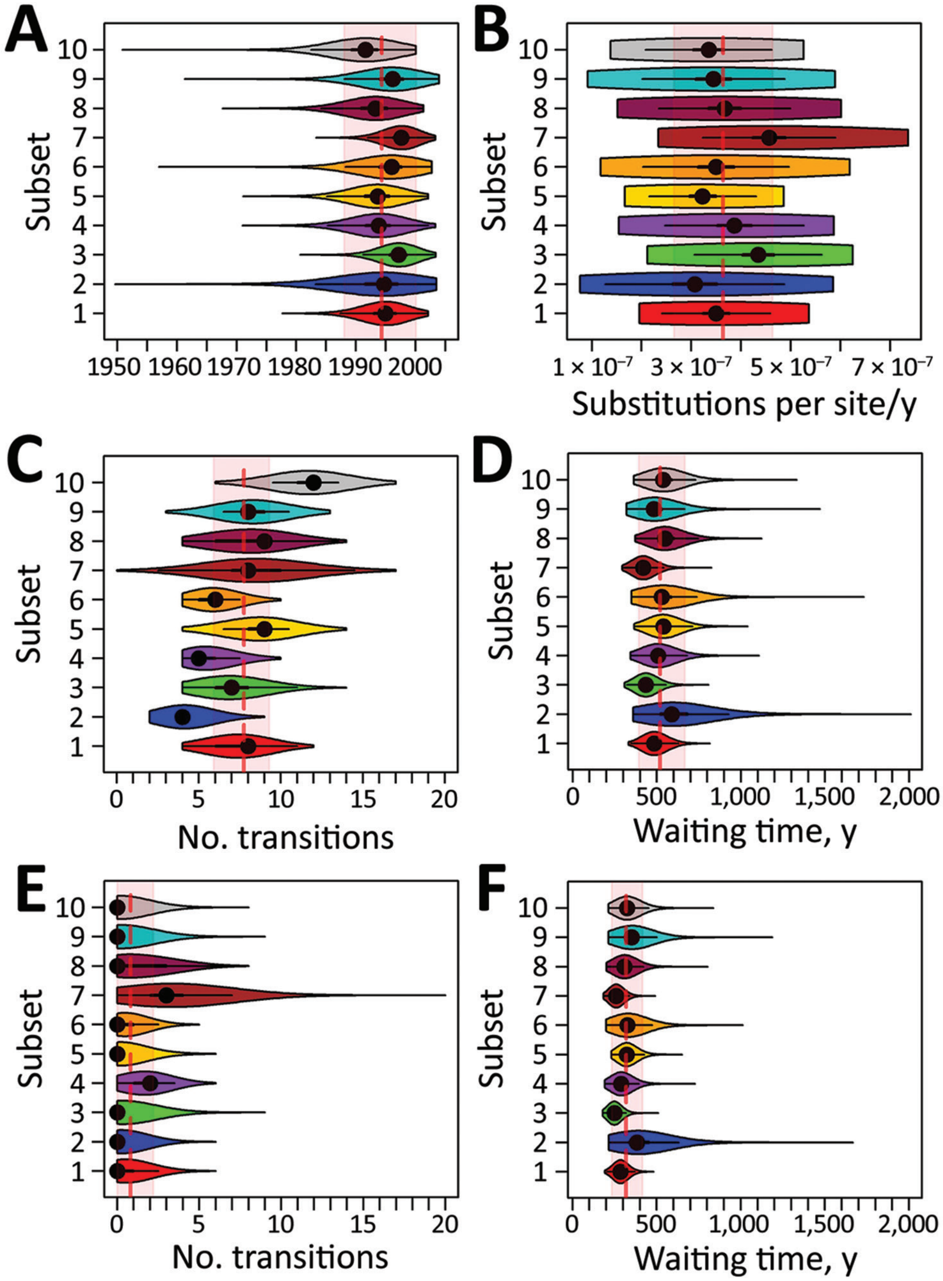

Figure 2. Summary of posterior estimates of all 10 subsets of sequences of *Salmonella enterica* subspecies *enterica* 4,[5],12:i:- sequence type (ST) 34 collected from multiple sources in the United States and Europe during 2008–2017. A) Inferred time (year) of the most recent common ancestor of the emerging *Salmonella* 4,[5],12:i:- ST34 clade. B) Estimated mutation rate (uncorrelated log-normally distributed mean parameter). C–F) Number of unobserved transitions from Europe to the United States (C) and United States to Europe (E) along each branch (Markov jumps) and total phylogenetic tree length spent (Markov rewards) in Europe (D) and the United States (F). Violin plots illustrate the posterior distribution and probability density of each subset. Dashed red vertical lines indicate average posterior value; red shaded areas indicate average 95% highest posterior density credible interval of all subsets.

States. The exponential growth rate of the population was estimated at 0.316/year (averaged across all subset means; Figure 1). In addition, the estimated (averaged) main introduction into the United States was 2004 (95% HPD 2000–2006; Appendix 2 Table 1). The occurrence of several additional smaller introductions was suggested by 48 sequences (6 from Europe and 42 from the United States). The 6 sequences from Europe were recovered from human sources; among sequences from the United States, 28 were from humans, 5 from food products, 6 from livestock, and 3 from other sources. Information on recent international travel was obtained for 22/28 of US isolates from humans, 2 of whom had traveled (1 to the Philippines and the other to France [S. Meyer et al., Minnesota Department of Health, pers. comm., 2019 Sep 23]).

Among the 1,431 *Salmonella* 4,[5],12:i:- ST34 sequences, 978 (68.34%) had genetic determinants contributing to the ASSuT profile, 108 (7.55%) conferred resistance to quinolones, and 82 (5.73%) conferred resistance to extended-spectrum cephalosporins. The probability of harboring most predominant acquired antimicrobial resistance genes (AARGs) conferring the resistance phenotypes described above was significantly higher for

Table. Association between collection location and presence of resistance genetic determinants in sequences of *Salmonella enterica* subspecies *enterica* serotype 4,[5],12:i:- sequence type 34 isolates collected in Europe and the United States, 2008–2017*

Conferring resistance to	Presence of genetic resistance determinants	No. positives/total (%) Europe	No. positives/total (%) United States	Odds ratio (95% CI), United States vs. Europe	p value†
ASSuT	ASSuT‡	406/690 (58.84)	572/741 (77.19)	2.37 (1.87–3.00)	**<0.001**
Extended-spectrum cephalosporins	$bla_{\text{CTX-M}}$ genes§	4/690 (0.58)	14/741 (1.89)	3.30 (1.03–13.84)	0.032
	$bla_{\text{CMY-2}}$	2/690 (0.29)	37/741 (4.99)	18.06 (4.63–155.09)	**<0.001**
	$bla_{\text{SHV-12}}$	0/690¶	27/741 (3.64)	53.15 (3.24–873.11)	**<0.001**
Quinolones	*qnrB19*	9/690 (1.3)	51/741 (6.88)	5.59 (2.70–13.01)	**<0.001**
	qnrB2	0/690¶	20/741 (2.7)	39.24 (2.36–650.05)	**<0.001**
	qnrS1	6/690 (0.87)	13/741 (1.75)	2.03 (0.72–6.57)	0.22
	aac(6')-Ib-cr	1/690 (0.14)	19/741 (2.56)	18.11 (2.86–751.91)	**<0.001**

*ASSuT indicates ampicillin, streptomycin, sulfonamides, and tetracycline.

†A statistically significant *p value* (boldface) is <0.05/8 = 0.00625 (adjusted for multiple comparisons using Bonferroni's correction).

‡Simultaneous presence of $bla_{\text{TEM-1}}$, *strA*, *strB*, *sul2*, and *tet(B)* genes (Appendix 2, https://wwwnc.cdc.gov/EID/article/26/12/20-0336-App2.pdf).

§Including $bla_{\text{CTX-M-1}}$ (n = 1), $bla_{\text{CTX-M-14}}$ (n = 2), $bla_{\text{CTX-M-55}}$ (n = 14), and $bla_{\text{CTX-M-65}}$ (n = 1).

¶Haldane-Anscombe correction (adding 0.5 to all 4 cells) was used to account for cells with a value of 0.

sequences of US isolates (odds ratio 2.37–26.05; Table). Yet associations between the collection location and the presence of $bla_{\text{CTX-M}}$ or *qnrS1* genes were not significant (Table). In addition, AARGs conferring resistance to colistin (*mcr*-1/*mcr*-3/*mcr*-5; Appendix 1) were detected in isolates from Europe only (n = 5).

Conclusions

Salmonella 4,[5],12:i:- ST34 was introduced into the United States from Europe on multiple occasions since the beginning of the 21st century. The main introduction occurred in 2004; additional independent introductions resulted in small clades for which the predominant sources were human travelers and imported food products. Human travelers (*6*) and imported food products (*7*) have been described as potential vehicles for introduction of salmonellae.

The date of introduction of the main clade into the United States is later than the first peer-reviewed report of a *Salmonella* 4,[5],12:i:- infection in the country in 1998 (*2*). However, given the antimicrobial susceptibility profile of isolates from that report (mostly not ASSuT) (*2*), they most likely belonged to the nonemerging ST19 clade, which was described elsewhere (*4*). In addition, the incidence of *Salmonella* 4,[5],12:i:- in humans increased only modestly (9.5%) during 2006–2011 but increased dramatically (78.3%) during 2011–2016 (*8*). A similar increase in detection after 2011 was described for clinical cases in swine from the midwestern United States (*9*). The difference between the date of main introduction into the United States found in this study and the later sharp increase in its prevalence in animals and humans may in part result from changes in reporting practices and increasing awareness (*8*). However, the increase since 2011 can be the result of rapid propagation of the ST34 population, possibly associated with swine (*4*). Moreover, White et al. (*10*) recently reported that according to the National Antibiotic Resistance Monitoring System, the percentage of ASSuT-resistant *Salmonella* 4,[5],12:i:- from humans increased from 17% in 2009 to 59.1% in 2015 (out of all *Salmonella* 4,[5],12:i:- clinical isolates from humans). This increase probably resulted to a large extent from ST34 strains, in which this phenotype is predominant. The estimated exponential yearly growth rate determined in our model (0.316/year), which corresponds to a population doubling time of 2.2 years, is in agreement with this dramatic increase of the ST34 population.

The presence of AARGs conferring resistance to quinolones and extended-spectrum cephalosporins has mainly been observed since 2014 and may be biased by the lack of sequences before 2013 (Appendix 2 Figure 12). Yet AARGs conferring resistance to quinolones were not found in *Salmonella* 4,[5],12:i:- ST34 strains from Europe collected before 2010 (*1*), and therefore our findings may reflect an increasing prevalence of these resistance determinants. Given time and overall unidirectionality of *Salmonella* 4,[5],12:i:- ST34 transmission from Europe to the United States, it is likely that the acquisition of AARGs to quinolones occurred independently in the United States and in Europe. Yet introduction of resistant strains from the United States to Europe is also possible. Contributors to the acquisition of resistance in the United States might be the approval for enrofloxacin use in swine in the United States since 2008 (*11*) and the potential dissemination of plasmids harboring AARGs to quinolones between *Salmonella* serotypes (*12*). Independent acquisition of resistance to quinolones by *Salmonella* in Asia has also been suggested (*13*). The presence of *mcr* resistance genes conferring resistance to colistin in sequences from Europe (n = 5) is alarming, given their recent worldwide spread (*14*). However, further investigation of the travel history associated with these cases may be required because the acquisition of *mcr* genes may be travel associated (*15*). The spread of *Salmonella* 4,[5],12:i:- ST34 from Europe to the United States and the presence of plasmid-mediated resistance genes to key antimicrobial classes such as quinolones, extended-spectrum cephalosporins, and colistin in this clade further highlights its potential risk to public health and emphasizes the need for robust surveillance and mitigation programs for such transboundary pathogens.

Acknowledgments

We thank staff members from the Minnesota Department of Health Foodborne, Waterborne, Vectorborne, and Zoonotic Diseases Section for providing the travel history records and for their advice on this work.

This work was supported by the Global Food Venture-MnDRIVE Initiative, the National Institute of Food and Agriculture (Animal Health Formula Fund project MIN-62-091) of the US Department of Agriculture, the Rapid Agricultural Response Fund, and the Swine Disease Eradication Center at the University of Minnesota. In addition, the United States-Israel Binational Agricultural Research and Development Fund awarded a Vaadia-BARD postdoctoral fellowship (no. FI-565-17) to E.E. A.E.M. is a Food Standards Agency research Fellow and is supported by the Biotechnology and Biological Sciences Research Council Institute Strategic Programme Microbes in the Food Chain BB/R012504/1 and its constituent project BBS/E/F/000PR10348 (Theme 1, Epidemiology and Evolution of Pathogens in the Food Chain). The Ramón y Cajal postdoctoral contract from the Spanish Ministry of Economy, Industry and Competitiveness (MINECO) (RYC-2016-20422) was awarded to J.A.

About the Author

Dr. Elnekave is a veterinarian and epidemiologist who has been working as a postdoctoral fellow in the Veterinary Population Medicine Department, University of Minnesota, and is a faculty member in the Koret School of Veterinary Medicine at the Robert H. Smith Faculty of Agricultural, Food and Environmental Sciences at the Hebrew University of Jerusalem, Israel. His primary research interest is the epidemiology of bacterial foodborne pathogens. He uses genetic tools and Bayesian models to study pathogen emergence, evolution, and antimicrobial resistance.

References

1. Petrovska L, Mather AE, AbuOun M, Branchu P, Harris SR, Connor T, et al. Microevolution of monophasic *Salmonella* Typhimurium during epidemic, United Kingdom, 2005–2010. Emerg Infect Dis. 2016;22:617–24. https://doi.org/10.3201/eid2204.150531
2. Agasan A, Kornblum J, Williams G, Pratt CC, Fleckenstein P, Wong M, et al. Profile of *Salmonella enterica* subsp. enterica (subspecies I) serotype 4,5,12:i:- strains causing food-borne infections in New York City. J Clin Microbiol. 2002;40:1924–9. https://doi.org/10.1128/JCM.40.6.1924-1929.2002
3. Centers for Disease Control and Prevention. National *Salmonella* surveillance overview. Atlanta: US Department of Health and Human Services; 2011.
4. Elnekave E, Hong S, Mather AE, Boxrud D, Taylor AJ, Lappi V, et al. *Salmonella enterica* serotype 4,[5],12:i:- in swine in the United States midwest: an emerging multidrug-resistant clade. Clin Infect Dis. 2018;66:877–85. https://doi.org/10.1093/cid/cix909
5. Drummond AJ, Rambaut A. BEAST: Bayesian Evolutionary Analysis by Sampling Trees. BMC Evol Biol. 2007;7:214. https://doi.org/10.1186/1471-2148-7-214
6. Williamson DA, Lane CR, Easton M, Valcanis M, Strachan J, Veitch MG, et al. Increasing antimicrobial resistance in nontyphoidal *Salmonella* isolates in Australia from 1979 to 2015. Antimicrob Agents Chemother. 2018;62:e02012-17. https://doi.org/10.1128/AAC.02012-17
7. Gould LH, Kline J, Monahan C, Vierk K. Outbreaks of disease associated with food imported into the United States, 1996–2014. Emerg Infect Dis. 2017;23:525–8. https://doi.org/10.3201/eid2303.161462
8. Centers for Disease Control and Prevention. National *Salmonella* surveillance annual report, 2016: Atlanta: US Department of Health and Human Services; 2018.
9. Hong S, Rovira A, Davies P, Ahlstrom C, Muellner P, Rendahl A, et al. Serotypes and antimicrobial resistance in *Salmonella enterica* recovered from clinical samples from cattle and swine in Minnesota, 2006 to 2015. PLoS One. 2016; 11:e0168016. https://doi.org/10.1371/journal.pone.0168016
10. White PL, Green AL, Holt KG, Hale KR. Multidrug-resistant *Salmonella enterica* subspecies I serovar 4,[5],12:i:- isolates recovered from Food Safety and Inspection Service-regulated products and food animal ceca, 2007-2016. Foodborne Pathog Dis. 2019;16:679–86. https://doi.org/10.1089/fpd.2018.2573
11. Food and Drug Administration. NADA 141–068 in the approved animal drug products (Green Book) [cited 2020 Aug 31]. https://animaldrugsatfda.fda.gov/adafda/views/#/home/previewsearch/141-068
12. Elnekave E, Hong SL, Lim S, Hayer SS, Boxrud D, Taylor AJ, et al. Circulation of plasmids harboring resistance genes to quinolones and/or extended-spectrum cephalosporins in multiple *Salmonella enterica* serotypes from swine in the United States. Antimicrob Agents Chemother. 2019;63:e02602-18. https://doi.org/10.1128/AAC.02602-18
13. Mather AE, Phuong TLT, Gao Y, Clare S, Mukhopadhyay S, Goulding DA, et al. New variant of multidrug-resistant *Salmonella enterica* serovar Typhimurium associated with invasive disease in immunocompromised patients in Vietnam. MBio. 2018;9:e01056-18. https://doi.org/10.1128/mBio.01056-18
14. McEwen SA, Collignon PJ. Antimicrobial resistance: a One Health perspective. Microbiol Spectr. 2018;6.
15. Arnott A, Wang Q, Bachmann N, Sadsad R, Biswas C, Sotomayor C, et al. Multidrug-resistant *Salmonella enterica* 4,[5],12:i:- sequence type 34, New South Wales, Australia, 2016–2017. Emerg Infect Dis. 2018;24:751–3. https://doi.org/10.3201/eid2404.171619

Address for correspondence: Ehud Elnekave, Koret School of Veterinary Medicine, Robert H. Smith Faculty of Agricultural, Food and Environmental Sciences, The Hebrew University, PO Box 12, Rehovot 76100, Israel; email: ehud.elnekave@mail.huji.ac.il or udie79@gmail.com

Article DOI: https://doi.org/10.3201/eid2612.200336

Transmission of Multidrug-Resistant *Salmonella enterica* Subspecies *enterica* 4,[5],12:i:- Sequence Type 34 between Europe and the United States

Appendix 2

Study population

The metadata of 1431 *Salmonella enterica* serotype 4,[5],12:i:- of sequence type (ST)34 isolates collected in USA (from multiple states) and Europe (mainly from United Kingdom and Denmark; TableS1) from 2008 through 2017 (excluding years 2011 and 2012) was obtained through various public sources (see below). Overall, the analysis included sequences of 690 European isolates and 741 isolates from USA (of which 73%, 10%, 4% and 13%, and 61%, 15%, 20% and 4% were recovered from humans, food products, livestock and other sources in Europe and USA, respectively). Availability of sequences from both USA and Europe on a certain collection year was set as a selection criterion to prevent potential bias of representing historic samples from a single location. In addition, when available, the sequences full collection date was used. Mid-year or mid-month were used as proxy when only the year or the year and month of collection were available, respectively. The study sequences were mainly identified using the National Center for Biotechnology Information (NCBI) 'pathogen detection' platform (https://www.ncbi.nlm.nih.gov/pathogens/; accessed: October 2017) (n=1162/1431). Additional sequences were found using the European Bioinformatics Institute (EMBL-EBI; https://www.ebi.ac.uk/) website (n=196/1431) and a recent study on *S.* 4,[5],12:i:- in USA (n=73/1431) (*1*).

Similar number of samples from each location-year combination were analyzed to avoid possible temporal and/or spatial selection biases that could affect the outcome of the analysis. Therefore, 50 sequences from years in which sequences were available from only one location were excluded from the analysis. This has further decreased the number of *S.* 4,[5],12:i:- ST34 sequences that were collected before 2013 and were available in the NCBI repository (Appendix 2, Figure 12), which may have limited the temporal signal in the dataset and biased the sample selection for the different subsets. Moreover, with the exception of *S*. 4,[5],12:i:- ST34 sequences from Vietnam, for which a European origin was previously suggested (*2*), there is limited availability of *S*. 4,[5],12:i:- ST34 sequences from world regions other than USA and Europe (mainly from United Kingdom and Denmark), and from non-human samples. Therefore, we could not assess the importance of other locations (different from USA and Europe) or to demonstrate the transmission of the pathogen between sources, respectively. However, despite these limitations, we were able to include 33% of the available *S*. 4,[5],12:i:- ST34 study population initially considered and to consistently demonstrate in multiple random subsets the possible directionality of transmission from Europe into USA (see text). The agreement with a preceding study in which a similar conclusion was obtained based on genetic similarities between *S*. Typhimurium and its monophasic variant from USA and Europe (*1*) further supports our findings.

Data analysis

Time-scaled phylogeny and discrete trait analysis

Bayesian Evolutionary Analysis Sampling Trees (BEAST v1.8.4 (*3*)) was used for estimation of divergence times, mutation rates and location trait transitions.

Subsets selection

Ten subsets of 112 sequences were selected for a time scaled analysis. To minimize the impact of potential spatial and temporal biases on the analysis outcome, the data was first stratified by collection location (Europe and USA) and by collection year. Then, an equal number of sequences from each location-year combination were randomly selected from the available sequences (up to ten sequences from each location-year combination) for each subset. Overall 474/1431 sequences were included in the selected subsets, of which 129 (27.2%), 233 (49.2%), 43 (9.1%), 35 (7.4%), 13 (2.7%), 7 (1.5%), 8 (1.7%), 1 (0.2%) and 5 (1.1%) were represented in a single, two, three, four, five, six, seven, eight and ten of the subsets, respectively.

Data filtering and quality control

Paired-end Illumina reads were downloaded from the NCBI repository and read quality was assessed using FASTQC (v0.11.6 (*4*)). De novo genome assemblies were constructed using the SPAdes assembler (v3.12.0) with the '--careful' option (*5*)). When necessary, the 'repair.sh' command in BBmap (*6*) was used to fix disordered raw reads before reassembly. The quality of contigs was assessed using QUAST (v4.6.3 (*7*)). Only sequences for which the N50 of assembled contigs was at least 30,000 nucleotides were further analyzed. SRR3322114 had a low N50 (10,567) yet was mistakenly included in the analysis (subsets 5 and 7). However, the inclusion of this single sequence is unlikely to affect the outcome, as also demonstrated by the similar outcomes of the multiple subsets used. In addition, the *Salmonella* In Silico Typing Resource (SISTR) v1.0.2 (*8*) was used only on 67% of the assemblies. However, we found that 96% of the in silico predicted serotype agreed with the reported serotype (the remaining 4% were removed from the analysis). Therefore, the represented population consisted of mainly 4,[5],12:i:- and not the diphasic ST34. In addition, the quality of all contigs from the *de novo* genome assemblies of the selected subsets (n=474 sequences) was further assessed: Bowtie2 (v2.3.4.1 (*9*)) was used to align the raw reads to the contigs and BBmap (v38.06 (*6*)) was used to calculate the average coverage depth of the contigs. Only sequences in which the average coverage depth of the contigs was at least 20 were included in further analysis.

Temporal signal

Reconstruction of maximum likelihood (ML) phylogeny trees for each subset was conducted for a priori estimation of the 'temporal signal' of the data. Raw reads were mapped to the reference *S.* 4,[5],12:i:- genome strain S04698-09 (RefSeq NZ_LN999997) using bowtie2 (v2.3.4.1 (*9*)) with default parameters. SAM files were compressed into BAM and sorted using 'view' and 'sort' commands from SAMtools (v1.3 (*10*)). Candidate single nucleotide polymorphisms (SNPs) were identified by using SAMtools (v1.3 (*10*)) and VarScan2 (v2.3.9 (*11*)). For each BAM alignment, a pileup file was created using 'mpileup' command from SAMtools (*10*), and only high quality SNPs were selected using 'mpileup2snp' command from VarScan2 (*11*) with the following criteria: a coverage threshold of 8, a minimum average base quality (Phred quality score) of 30, and a 90% agreement threshold. SNPs found using this method were output in variant call format and were parsed and examined. Phage regions were detected in the reference genome using PHASTER (*12*) and SNPs within such regions were masked using a custom python script (below – script 1). Recombination regions were identified using Gubbins (v2.3.2 (*13*)). Duplicate sequences (i.e. different isolates but genetically identical) were removed using a custom python script (below –script 2). Phylogenetic ML tree reconstruction was conducted for each subset separately using RAxML (v8.2.10 (*14*)) with the following definitions: a general time reversible substitution evolutionary model with gamma correction (GTR+Γ), 250 rapid bootstrap replicates and four randomly generated rapid bootstrap seeds. The best tree was selected based on the maximum likelihood and all bootstrap trees were concatenated into a single file containing the 1000 bootstrap trees.

The ML phylogenetic trees were used for estimating the ‘Temporal signal’ by generating a linear regression of phylogenetic root-to-tip distances against the sampling dates using Tempest (v1.5 (*15*)). All subsets demonstrated a positive correlation between root-to-tip distances and sampling dates in all subsets (R^2=0.21-0.27).

Model selection

A single subset (subset 2) was arbitrarily selected for the model selection process (including the discrete trait model selection) and the final model combination was applied to all ten subsets.

A general time reversible (GTR) substitution model was selected using Jmodeltest (v2.1.10) (*16*,*17*). Different combinations of molecular clocks (i.e. strict or uncorrelated lognormal relaxed) and population growth models [i.e., constant, logistic, exponential, or Gaussian Markov random field (GMRF) Bayesian skyride] were evaluated. Each model combination was tested in two independent Markov chain-Monte Carlo (MCMC) runs of at least 200 million iterations, with sampling every 20,000 iterations. Convergence and proper mixing of all MCMC runs (ensuring an effective sample size > 200) and agreement between the independent MCMC runs for each model were verified manually using Tracer (v1.7.1 (*18*)) after excluding 10% of the MCMC run as burn-in. The log marginal likelihoods for each model were obtained using path sampling (PS)/stepping-stone sampling (SS) (see below) and the models were compared by calculating the Bayes factors (*19*,*20*). The combination of GTR substitution rates, uncorrelated lognormal relaxed molecular clock, and exponential growth demographic model had the highest log Bayes factor value and was chosen as the model specification for further analyses.

In addition to the ‘temporal signal’ analysis with Tempest (above), at this stage, a tip-date randomization test was conducted (with the selected model combination) using the package ‘TipDatingBeast’ (v1.0.6 (*21*)) in R (v3.4.3 (*22*)), and the evaluated time to most recent common ancestor (TMRCA) and mutation rate values were compared between the real data and the randomized trials (n=20). This further support the temporal structure of the data as no overlap was found between the highest posterior density $(\mathrm{HPD})_{95\%}$ credible intervals and mean values of the randomized trials (n=20) and real data, respectively, for time to the most recent common ancestor (TMRCA) and mutation rates (Appendix 2 Figure 13).

Discrete trait analysis

Bayesian phylogeographic reconstruction was conducted by incorporating the ‘collection location’ trait under a discrete trait geospatial model (*23*) using the model combination found in the previous step. Symmetric and asymmetric models for trait transition were considered. Each model combination was tested as described above. The combination of GTR substitution rates, uncorrelated lognormal relaxed molecular clock, and exponential growth with asymmetric trait transitions was selected in this step.

This model combination was then used with all remaining subsets (at least two independent runs of 200 million iterations or more were run for each). The directionality of the spatial diffusion process was examined by calculating the ‘collection location’ Markov jumps (estimates the expectations for state transitions from USA to Europe and from Europe to USA) and Markov rewards (waiting times; estimate the expectations for time that is spent in each location, Europe or USA) (*24*,*25*). We found that the transmission was predominantly unidirectional, as reflected by the high number of Markov jumps from Europe to USA and the long waiting periods (Markov rewards) in Europe (see text).

In all analyses, the independent MCMC run outputs (log and trees files) of each model were combined using LogCombiner (v1.8.4 (*3*)), after exclusion of a 10% burn-in period. TreeAnnotator (v1.8.4 (*3*)) was used for selection and annotation of a single maximum clade credibility tree (using common ancestor node heights).

In all models, a mutation rate of 3.4×10^{-7} substitutions per site per year, previously estimated for *S*. Typhimurium DT104 (*26*), was set as the mean value for a lognormal prior distribution of the clock rate (with standard deviation (stdev)=2). In addition, a lognormal distribution (mean=10 and stdev=2.148) was set as prior population size. In addition to the priors described above, for logistic population growth models a Laplace distribution (mean=0, stdev=0.026568; initial value=0.26) was set as a prior. In order to avoid the potential ascertainment bias as only the variable site alignments were used in the analysis (ranged between 1195 and 1465 sites in the ten subsets), the total number of nucleotides in the reference genome (RefSeq NZ_LN999997; 1204735, 1315079, 1312718 and 1204706 for A, C, G & T, respectively) were incorporated in the xml file as an approximation of the non-variable sites in the analysis. The following text:

```
<patterns id="patterns" from="1" strip="false">
        <alignment idref="alignment"/>
    </patterns>
```

Was replaced with:

```
<mergePatterns id="patterns">
 <patterns from="1" every="1">
 <alignment idref="alignment"/>
 </patterns>

 <constantPatterns>
 <alignment idref="alignment"/>
 <counts>
 <parameter value="1204735 1315079 1312718 1204706"/>
 </counts>
 </constantPatterns>
 </mergePatterns>
```

In addition, for estimating the time of the main introduction into USA, the clade’s ancestral node was visually identified in each of the ten subsets maximum clade credibility trees and the node height and high posterior density 95% (HPD$_{95\%}$) were recorded and the average value for all subsets were calculated (Appendix 2 Table 1 and Figures 1-10) .

Moreover, the analysis of subset 2 (without the discrete trait analysis) was repeated (with two independent seeds) while sampling only from the prior, to verify that prior parameters were not over-constraining the calculations.

In all models, The log marginal likelihoods for the model were obtained using path sampling (PS) / stepping-stone sampling (SS) (for both PS and SS - 100 paths were used, and the number of PS/SS iterations was equal to number of MCMC iterations in the analysis divided by the number of PS/SS paths) and the models were compared by calculating the Bayes factors (*19*,*20*).

Association-index (AI)

Evaluation and quantification of the correlation between the location trait and shared ancestry was done using the Bayesian Tip-association Significance testing (BaTS v0.9.0) (*27*) software. Briefly, the software calculates the AI for each tree in the posterior distribution of the real data and for permutations in which the traits are randomly assigned to the tree tips. The latter will serve as the null hypothesis, in which there is no association between the trait and ancestry. A posterior distribution of AI statistic is formed for the real data and for the permutations. The test significance is obtained by calculating the proportion of the mean posterior estimate for the permutations that are extreme than the mean posterior for the real data. The trait-ancestry correlation was estimated (using 1,000 permutations) for each of the ten subsets in this analysis and found statistically significant ($p<0.05$; Appendix 2 Table 2) with an average ratio of 0.12 ($HPD_{95\%}$: 0.11-0.14), suggesting an association between the sampling locations and the tree phylogeny.

Potential additional introductions

In addition to the main introduction from Europe to USA, the maximum clade credibility trees of all subsets were visually scanned to detect a few sequences (up to five in a monophyletic group) intermingled with sequences from a different location (i.e. European sequences located within USA main clade and/or USA sequences that were not part of USA main clade; Appendix 2 Figures 1-10), which can potentially indicate additional introductions. Sequence details were summarized and further investigation of potential travel history records was conducted. Overall, 48 sequences (6 from Europe and 42 from USA) that represent potential additional introductions (between 4 and 14 sequences were included in each subset – Appendix 2, Table 4) were identified. The six European sequences were recovered from human sources and 28, 5, 6 and 3 of USA sequences were recovered from humans, food products, livestock and other sources, respectively. History of recent international travel information was obtained for 22/28 of USA human isolates, of which information was not available for six (cases were not interviewed), 14 had not traveled recently and two had recently traveled: one became ill while traveling to the Philippines and the other was travelling to France for three days in the week before showing clinical signs (personal communication - Minnesota Department of Health).

Sequence typing and acquired antimicrobial resistance genes

De novo genome assemblies were constructed using SPAdes (v3.12.0 (*5*)). Acquired antimicrobial resistance genes (AARGs) and Multi Locus Sequence types (MLST) were identified using ResFinder (v2.1 (*28*)) and MLST; v1.6 (*29*)) tools from the 'bacterial analysis pipeline' in the Center for Genomic Epidemiology server (https://cge.cbs.dtu.dk/services/cge/). All tools and their databases were downloaded and installed on a local server (March 2018) and used with the 'bacterial analysis pipeline' default settings. Outcomes were combined in a tab-separated file using python (www.python.org) pandas package (v0.23.4 (*30*)).

The simultaneous presence of genotypic resistance to ampicillin, streptomycin, sulfonamides, and tetracycline (ASSuT) was defined according to Elnekave et al. (*1*) as simultaneous presence of $\textit{bla}_{\text{TEM-1}}$, *strA*, *strB*, *sul2*, and *tet(B)* genes. However, the nomenclature of the genes in ResFinder was updated and therefore: *strB* gene was identified as *aph (6)-Id* gene; and *strA* gene was identified as *strA* or *aph(3'')-Ib* genes.

R (v3.4.3 (*22*)) was used to perform Pearson's chi-square or Fisher's exact tests [using package hypergea (v1.3.6 (*31*)) to incorporate the Haldane-Anscombe correction for zero values, when needed] for estimating associations between 'collection location', defined as USA or Europe, and: (i) the simultaneous presence of genotypic resistance to ASSuT; (ii) presence of predominant (found in at least 15 sequences) AARGs to quinolones; or iii) to extended spectrum cephalosporins (ESC; see text).

Data summarizing and visualization

The R packages ‘dplyr’ (v0.7.4 (*32*)), ‘stringr’ (v1.2.0 (*33*)) and ‘tidyr’ (v0.8.0 (*34*)) were used for data filtering and subset selection. Packages ‘vioplot’ (v0.3.0 (*35*)), ‘HDInterval’ (v0.2.0 (*36*)), ‘ggplot2’ (v2.2.1 (*37*)), ‘gridExtra’ (v2.3 (*38*)), ‘ggpubr’ (v0.2 (*39*)), ‘lubridate’ (v1.7.1 (*40*)) and ‘ggtree’ (v1.10.5 (*41*)) were used for output summary and visualization.

Phylogenetic ML tree reconstruction for the entire study population

In addition to the described analysis, to estimate whether the selected subsets are providing a good representation of the entire study population tree topology, a ML core genome phylogeny was reconstructed using all study isolates (n=1431). Core and pan genomes were obtained using the annotated [using Prokka (v1.13.3 (*42*))] assembled contigs in ‘Roary’ (v3.12.0 (*43*)) with an identity cut-off of 95%. Core genome ML tree reconstruction was conducted using RAxML (v8.2.10 (*14*)) (after removal of duplicates only 1185 sequences were included in the phylogeny tree; 25,687 variable sites were used for this analysis; Appendix 2, Figure 11) with a general time reversible substitution evolutionary model with gamma correction (GTR+Γ) and 1000 bootstrap replicates. Trees were rooted using *S*. Enteritidis isolates (SRR1965760 and SRR3242211). Packages ‘ape’ (v5.0 (*44*)) and ‘ggtree’ (v1.10.5 (*45*)) in R software (v3.4.3 (*22*)) were used for visualization.

Data availability

The raw XML and log files are available from the authors upon request.

References

1. Elnekave E, Hong S, Mather AE, Boxrud D, Taylor AJ, Lappi V, et al. Salmonella enterica Serotype 4,[5],12:i:- in Swine in the United States Midwest: An Emerging Multidrug-Resistant Clade. Clin Infect Dis. 2018;66:877–85. PubMed https://doi.org/10.1093/cid/cix909

2. Mather AE, Phuong TLT, Gao Y, Clare S, Mukhopadhyay S, Goulding DA, et al. New Variant of Multidrug-Resistant *Salmonella enterica* Serovar Typhimurium Associated with Invasive Disease in Immunocompromised Patients in Vietnam. MBio. 2018;9:e01056-18. PubMed https://doi.org/10.1128/mBio.01056-18

3. Drummond AJ, Rambaut A. BEAST: Bayesian evolutionary analysis by sampling trees. BMC Evol Biol. 2007;7:214. PubMed https://doi.org/10.1186/1471-2148-7-214

4. Andrews S. FastQC: a quality control tool for high throughput sequence data. 2010.

5. Bankevich A, Nurk S, Antipov D, Gurevich AA, Dvorkin M, Kulikov AS, et al. SPAdes: a new genome assembly algorithm and its applications to single-cell sequencing. J Comput Biol. 2012;19:455–77. PubMed https://doi.org/10.1089/cmb.2012.0021

6. Bushnell B. BBMap short-read aligner, and other bioinformatics tools.

7. Gurevich A, Saveliev V, Vyahhi N, Tesler G. QUAST: quality assessment tool for genome assemblies. Bioinformatics. 2013;29:1072–5. PubMed https://doi.org/10.1093/bioinformatics/btt086

8. Yoshida CE, Kruczkiewicz P, Laing CR, Lingohr EJ, Gannon VP, Nash JH, et al. The Salmonella In Silico Typing Resource (SISTR): An Open Web-Accessible Tool for Rapidly Typing and Subtyping Draft Salmonella Genome Assemblies. PLoS One. 2016;11:e0147101. PubMed https://doi.org/10.1371/journal.pone.0147101

9. Langmead B, Salzberg SL. Fast gapped-read alignment with Bowtie 2. Nat Methods. 2012;9:357–9. PubMed https://doi.org/10.1038/nmeth.1923

10. Li H, Handsaker B, Wysoker A, Fennell T, Ruan J, Homer N, et al.; 1000 Genome Project Data Processing Subgroup. The Sequence Alignment/Map format and SAMtools. Bioinformatics. 2009;25:2078–9. PubMed https://doi.org/10.1093/bioinformatics/btp352

11. Koboldt DC, Zhang Q, Larson DE, Shen D, McLellan MD, Lin L, et al. VarScan 2: somatic mutation and copy number alteration discovery in cancer by exome sequencing. Genome Res. 2012;22:568–76. PubMed https://doi.org/10.1101/gr.129684.111

12. Arndt D, Grant JR, Marcu A, Sajed T, Pon A, Liang Y, et al. PHASTER: a better, faster version of the PHAST phage search tool. Nucleic Acids Res. 2016;44(W1):W16-21. PubMed https://doi.org/10.1093/nar/gkw387

13. Croucher NJ, Page AJ, Connor TR, Delaney AJ, Keane JA, Bentley SD, et al. Rapid phylogenetic analysis of large samples of recombinant bacterial whole genome sequences using Gubbins. Nucleic Acids Res. 2015;43:e15. PubMed https://doi.org/10.1093/nar/gku1196

14. Stamatakis A. RAxML version 8: a tool for phylogenetic analysis and post-analysis of large phylogenies. Bioinformatics. 2014;30:1312–3. PubMed https://doi.org/10.1093/bioinformatics/btu033

15. Rambaut A, Lam TT, Max Carvalho L, Pybus OG. Exploring the temporal structure of heterochronous sequences using TempEst (formerly Path-O-Gen). Virus Evol. 2016;2:vew007. PubMed https://doi.org/10.1093/ve/vew007

16. Darriba D, Taboada GL, Doallo R, Posada D. jModelTest 2: more models, new heuristics and parallel computing. Nat Methods. 2012;9:772. PubMed https://doi.org/10.1038/nmeth.2109

17. Guindon S, Gascuel O. A simple, fast, and accurate algorithm to estimate large phylogenies by maximum likelihood. Syst Biol. 2003;52:696–704. PubMed https://doi.org/10.1080/10635150390235520

18. Rambaut A, Drummond AJ, Xie D, Baele G, Suchard MA. Posterior Summarization in Bayesian Phylogenetics Using Tracer 1.7. Syst Biol. 2018;67:901–4. PubMed https://doi.org/10.1093/sysbio/syy032

19. Baele G, Lemey P, Bedford T, Rambaut A, Suchard MA, Alekseyenko AV. Improving the accuracy of demographic and molecular clock model comparison while accommodating phylogenetic uncertainty. Mol Biol Evol. 2012;29:2157–67. PubMed https://doi.org/10.1093/molbev/mss084

20. Baele G, Li WL, Drummond AJ, Suchard MA, Lemey P. Accurate model selection of relaxed molecular clocks in bayesian phylogenetics. Mol Biol Evol. 2013;30:239–43. PubMed https://doi.org/10.1093/molbev/mss243

21. Rieux A, Khatchikian CE. tipdatingbeast: an r package to assist the implementation of phylogenetic tip-dating tests using beast. Mol Ecol Resour. 2017;17:608–13. PubMed https://doi.org/10.1111/1755-0998.12603

22. R Core Team. R: A language and environment for statistical computing. R Foundation for Statistical Computing. Vienna, Austria; 2016.

23. Lemey P, Rambaut A, Drummond AJ, Suchard MA. Bayesian phylogeography finds its roots. PLOS Comput Biol. 2009;5:e1000520. PubMed https://doi.org/10.1371/journal.pcbi.1000520

24. Minin VN, Suchard MA. Counting labeled transitions in continuous-time Markov models of evolution. J Math Biol. 2008;56:391–412. PubMed https://doi.org/10.1007/s00285-007-0120-8

25. Minin VN, Suchard MA. Fast, accurate and simulation-free stochastic mapping. Philos Trans R Soc Lond B Biol Sci. 2008;363:3985–95. PubMed https://doi.org/10.1098/rstb.2008.0176

26. Mather AE, Reid SW, Maskell DJ, Parkhill J, Fookes MC, Harris SR, et al. Distinguishable epidemics of multidrug-resistant Salmonella Typhimurium DT104 in different hosts. Science. 2013;341:1514–7. PubMed https://doi.org/10.1126/science.1240578

27. Parker J, Rambaut A, Pybus OG. Correlating viral phenotypes with phylogeny: accounting for phylogenetic uncertainty. Infect Genet Evol. 2008;8:239–46. PubMed https://doi.org/10.1016/j.meegid.2007.08.001

28. Zankari E, Hasman H, Cosentino S, Vestergaard M, Rasmussen S, Lund O, et al. Identification of acquired antimicrobial resistance genes. J Antimicrob Chemother. 2012;67:2640–4. PubMed https://doi.org/10.1093/jac/dks261

29. Larsen MV, Cosentino S, Rasmussen S, Friis C, Hasman H, Marvig RL, et al. Multilocus sequence typing of total-genome-sequenced bacteria. J Clin Microbiol. 2012;50:1355–61. PubMed https://doi.org/10.1128/JCM.06094-11

30. McKinney W. Data structures for statistical computing in python. Proceedings of the 9th Python in Science Conference; 2010: van der Voort S, Millman J; 2010. p. 51-6.

31. Boenn M. hypergea: Hypergeometric Tests. R package version 1.3.6. https://CRAN.R-project.org/package=hypergea; 2018.

32. Wickham H, Francois, R., Henry, L., Müller, K. dplyr: A Grammar of Data Manipulation. R package version 0.7.4. 2017.

33. Wickham H. stringr: Simple, Consistent Wrappers for Common String Operations. 2015 [cited; Available from: https://CRAN.R-project.org/package=stringr

34. Wickham H, Henry L. tidyr: Easily Tidy Data with 'spread()' and 'gather()' Functions. R package. 0.8.0 ed; 2018.

35. Adler D, Kelly ST. vioplot: violin plot. R package. 0.3.0 ed; 2018.

36. Meredith M, Kruschke J. HDInterval: Highest (Posterior) Density Intervals. R package 0.2.0 ed; 2018.

37. Wickham H. Ggplot2 : elegant graphics for data analysis. New York: Springer; 2009.

38. Auguie B. gridExtra: Miscellaneous Functions for "Grid" Graphics. R package version 2.3. 2017.

39. Kassambara A. ggpubr: 'ggplot2' Based Publication Ready Plots. R package version 0.2. 2018.

40. Grolemund G, Wickham H. Dates and times made easy with lubridate. J Stat Softw. 2011;40:1–25. https://doi.org/10.18637/jss.v040.i03

41. Yu G, Smith DK, Zhu H, Guan Y, Lam TTY. ggtree: an R package for visualization and annotation of phylogenetic trees with their covariates and other associated data. Methods Ecol Evol. 2017;8:28–36. https://doi.org/10.1111/2041-210X.12628

42. Seemann T. Prokka: rapid prokaryotic genome annotation. Bioinformatics. 2014;30:2068–9. PubMed https://doi.org/10.1093/bioinformatics/btu153

43. Page AJ, Cummins CA, Hunt M, Wong VK, Reuter S, Holden MT, et al. Roary: rapid large-scale prokaryote pan genome analysis. Bioinformatics. 2015;31:3691–3. PubMed https://doi.org/10.1093/bioinformatics/btv421

44. Paradis E, Claude J, Strimmer K. APE: Analyses of Phylogenetics and Evolution in R language. Bioinformatics. 2004;20:289–90. PubMed https://doi.org/10.1093/bioinformatics/btg412

45. Yu G, Smith DK, Zhu H, Guan Y, Lam TT-Y. ggtree: an r package for visualization and annotation of phylogenetic trees with their covariates and other associated data. Methods Ecol Evol. 2017;8:28–36. https://doi.org/10.1111/2041-210X.12628

Script 1 – Masking phage and recombinant regions

```
# filter_snps -r [regions file] -f [VCF file] -o [output folder]

# masks bases in a VCF file with locations specified in the regions file

import argparse

import pandas as pd

import os

def filter_phage(regions,pos,alt):

found = False

for i in range(len(regions)):

j=regions.ix[i]

if pos >= j.start and pos <= j.stop:

return 'N'

return alt

def main():

#argparse

parser = argparse.ArgumentParser()
```

```
parser.add_argument('-r','--regions',help='Input tab separated regions file (no header)',required=True)
parser.add_argument('-f','--file',help='Input vcf formatted SNPS file',required=True)
parser.add_argument('-o','--output',help='Output folder',required=True)
args=parser.parse_args()
outputfolder = args.output
vcfFile = args.file
regions = args.regions
name = vcfFile.split('/')[-1].split('.')[0]
#create output folder if it doesnt exist
if not os.path.exists(outputfolder):
os.mkdir(outputfolder)
regions=pd.read_csv(regions,sep='\t',names=['id','start','stop']).sort_values('start')
vcf = pd.read_csv(vcfFile,sep='\t',skiprows=23)
vcf['ALT']=vcf.apply(lambda row: filter_phage(regions,row['POS'], row['ALT']), axis=1)
with open(vcfFile) as myfile:
head = [next(myfile) for x in range (23)]
test=[]
test.append(vcfFile)
counts = vcf['ALT'].value_counts().to_dict()
#test.append(counts.get('A')+counts.get('T')+counts.get('C')+counts.get('G'))
print(counts)
with open(outputfolder+'/'+name+'_filtered.vcf','w') as newfile:
newfile.writelines(head)
```

```
vcf.to_csv(newfile,mode='a',sep='\t',index=False)
main()
```

Script 2 – Duplicates removal

```
import sys
from Bio import SeqIO
#clean.py [fasta file]
def sequence_cleaner(fasta_file, min_length=0, por_n=100):
# Create our hash table to add the sequences
sequences={}
# Using the Biopython fasta parse we can read our fasta input
for seq_record in SeqIO.parse(fasta_file, "fasta"):
# Take the current sequence
sequence = str(seq_record.seq).upper()
# Check if the current sequence is according to the user parameters
if (len(sequence) >= min_length and
(float(sequence.count("N"))/float(len(sequence)))*100 <= por_n):
# If the sequence passed in the test "is it clean?" and it isn't in the
# hash table, the sequence and its id are going to be in the hash
if sequence not in sequences:
sequences[sequence] = seq_record.id
# If it is already in the hash table, we're just gonna concatenate the ID
# of the current sequence to another one that is already in the hash table
else:
sequences[sequence] += "_" + seq_record.id
```

```
# Write the clean sequences
# Create a file in the same directory where you ran this script
output_file = open("clear_" + fasta_file, "w+")
# Just read the hash table and write on the file as a fasta format
for sequence in sequences:
output_file.write(">" + sequences[sequence] + "\n" + sequence + "\n")
output_file.close()
print("CLEAN!!!\nPlease check clear_" + fasta_file)
userParameters = sys.argv[1:]
try:
if len(userParameters) == 1:
sequence_cleaner(userParameters[0])
elif len(userParameters) == 2:
sequence_cleaner(userParameters[0], float(userParameters[1]))
elif len(userParameters) == 3:
sequence_cleaner(userParameters[0], float(userParameters[1]),
float(userParameters[2]))
else:
print("There is a problem!")
except:
print("There is a problem!")
```

Appendix 2 Table 1. The estimated time to the most recent common ancestor (TMRCA) of the main USA *S*. 4,[5],12:i:- ST34 clade in each subset. The ancestor node was visually identified* in each subset and an average value was calculated for all*

Subset	TMRCA - USA clade ($HPD_{95\%}$)
1	2005 (2002-2007)
2	2002 (1996-2007)
3	2006 (2004-2007)
4	2003 (2000-2006)
5	2003 (2001-2006)
6	2004 (2000-2007)
7	2006 (2004-2007)
8	2002 (1999-2005)
9	2001 (1995-2005)
10	2003 (2000-2006)
All (average)	2004 (2000-2006)

*The ancestor nodes are indicated in Appendix 2, Figures 1–10. $HPD_{95\%}$, highest posterior density 95% credible interval

Appendix 2 Table 2. The association index (AI) statistic mean of the real data and the randomized permutations* (the null hypothesis) for each of the ten subsets; and the AI ratio† between the real data and randomized permutations.

	Mean ($HPD_{95\%}$‡)			
Subset	Observed data	Null hypothesis (randomized permutations)	AI ratio	p value
1	0.49 (0.41-0.59)	5.95 (4.67-7.25)	0.08 (0.08-0.09)	0.0
2	0.37 (0.31-0.48)	5.91 (4.59-7.26)	0.06 (0.06-0.07)	0.0
3	0.48 (0.32-0.75)	5.36 (4.2-6.54)	0.09 (0.08-0.11)	0.0
4	0.68 (0.4-0.9)	5.75 (4.55-6.99)	0.12 (0.09-0.13)	0.0
5	0.76 (0.66-0.91)	6.06 (4.67-7.43)	0.13 (0.12-0.14)	0.0
6	0.62 (0.35-0.95)	6.19 (4.89-7.49)	0.1 (0.07-0.13)	0.0
7	0.99 (0.57-1.42)	5.69 (4.42-6.95)	0.17 (0.13-0.2)	0.0
8	0.58 (0.38-0.92)	6.03 (4.7-7.34)	0.1 (0.08-0.13)	0.0
9	0.96 (0.65-1.21)	6.07 (4.72-7.36)	0.16 (0.14-0.16)	0.0
10	1.28 (1.02-1.66)	6.19 (4.91-7.45)	0.21 (0.21-0.22)	0.0

*BaTS (v0. 9.0; (Appendix 2, ref. 26)) was used for calculating the AI and 1000 permutations were set in the analysis of each subset.

† AI mean of Real (observed) data / randomized permutations. Values closer to zero, rejects the null hypothesis (AI ratio = 1) and suggest association between location and ancestry (as was described by Mather et al. (Appendix 2, ref. 25))

‡ HPD95%= Highest posterior density 95% credible interval

Appendix 2 Table 3. The number sequences from potential additional introductions through travel/import identified in each subset*

	Collection location		
Subset	Europe	USA	Total
1	1	10	11
2		5	5
3		8	8
4	2	4	6
5		10	10
6	1	7	8
7	2	10	12
8		7	7
9		14	14
10		13	13
All	6	88	94

*Introductions in addition to the one leading to the main USA *S*. 4,[5],12:i:- ST34 clade (as described in the text); Some of the sequences are included in more than one subset. Overall, 48 unique sequences were identified as possible travel/import source for the additional introductions.

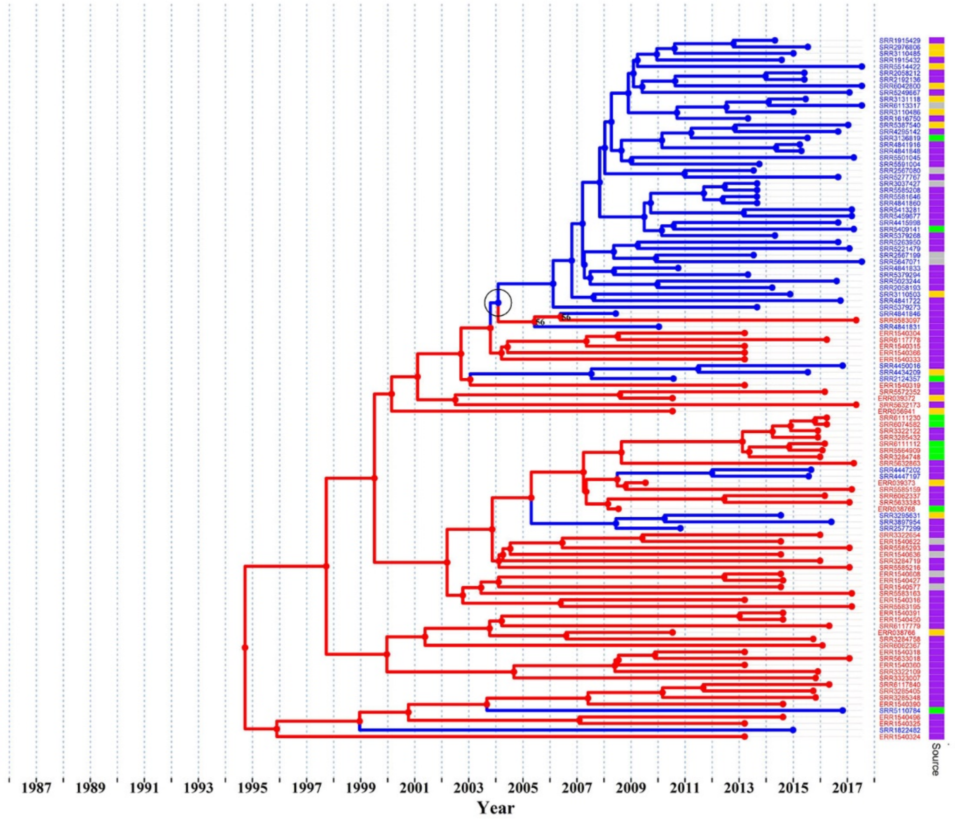
56
56
Source
1987
1989
1991
1993
1995
1997
1999
2001
2003
2005
2007
2009
2011
2013
2015
2017
Year

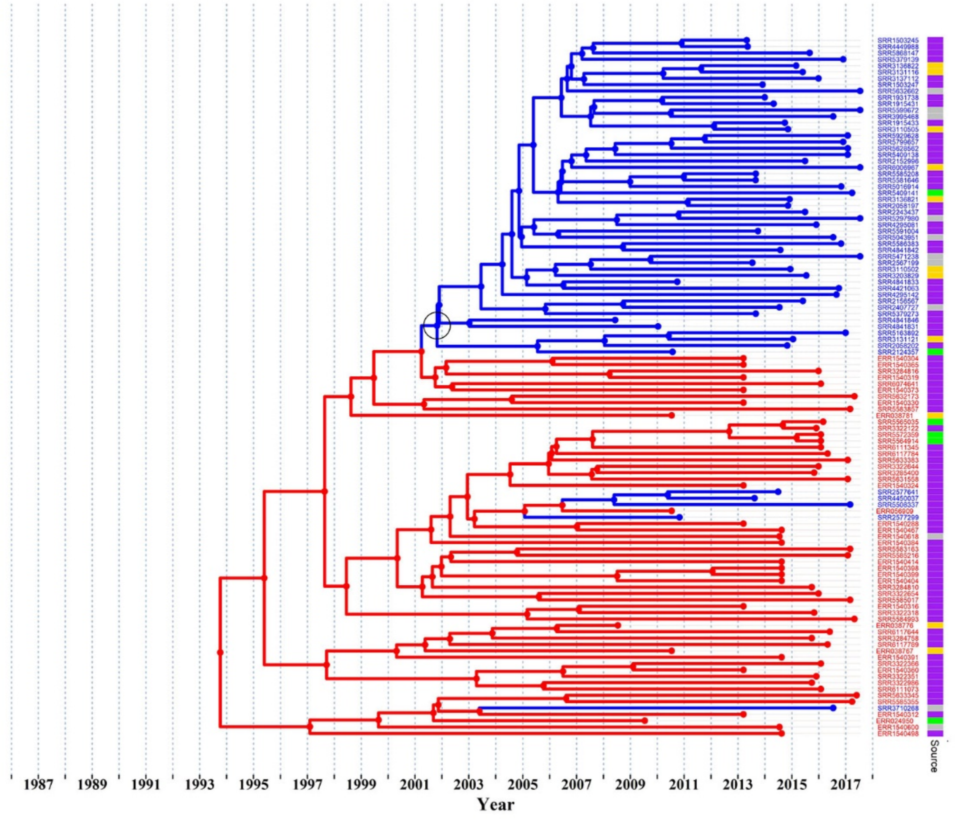
Source
1987
1989
1991
1993
1995
1997
1999
2001
2003
2005
2007
2009
2011
2013
2015
2017
Year

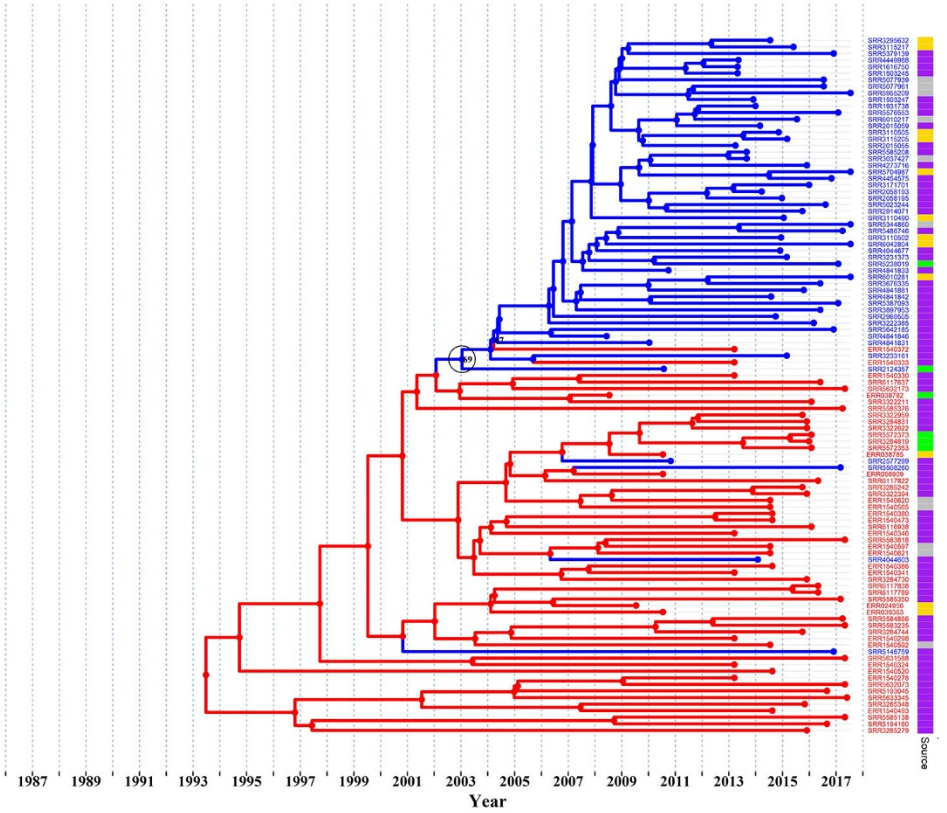
69
67
Source
1987
1989
1991
1993
1995
1997
1999
2001
2003
2005
2007
2009
2011
2013
2015
2017
Year

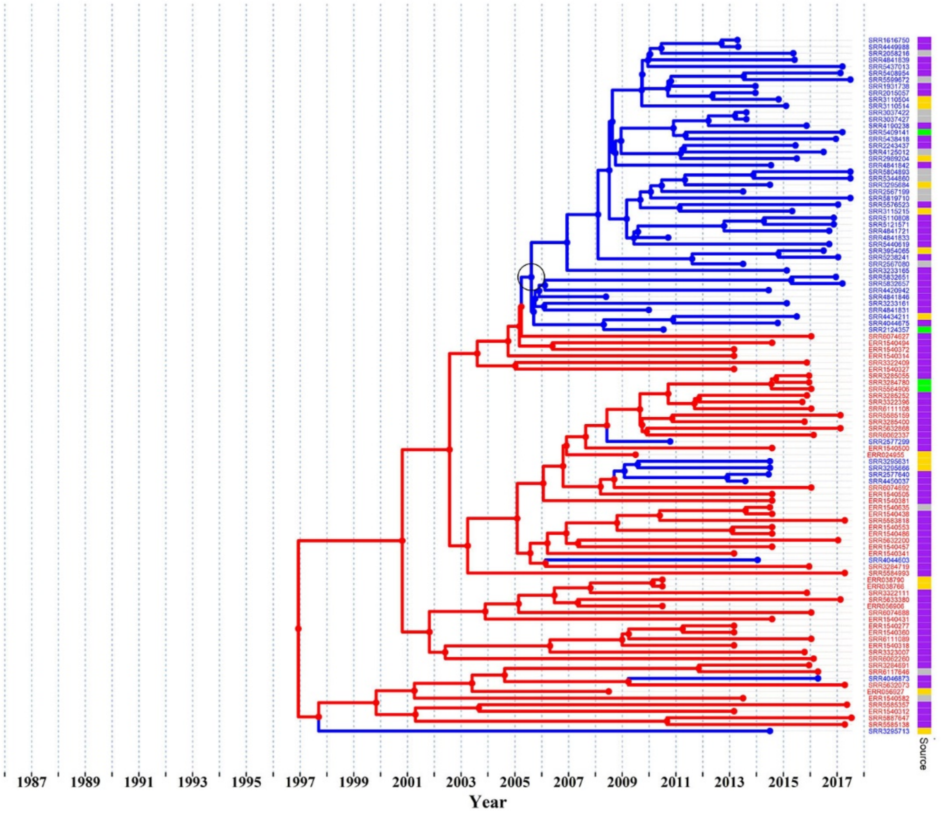
Source
1987
1989
1991
1993
1995
1997
1999
2001
2003
2005
2007
2009
2011
2013
2015
2017
Year

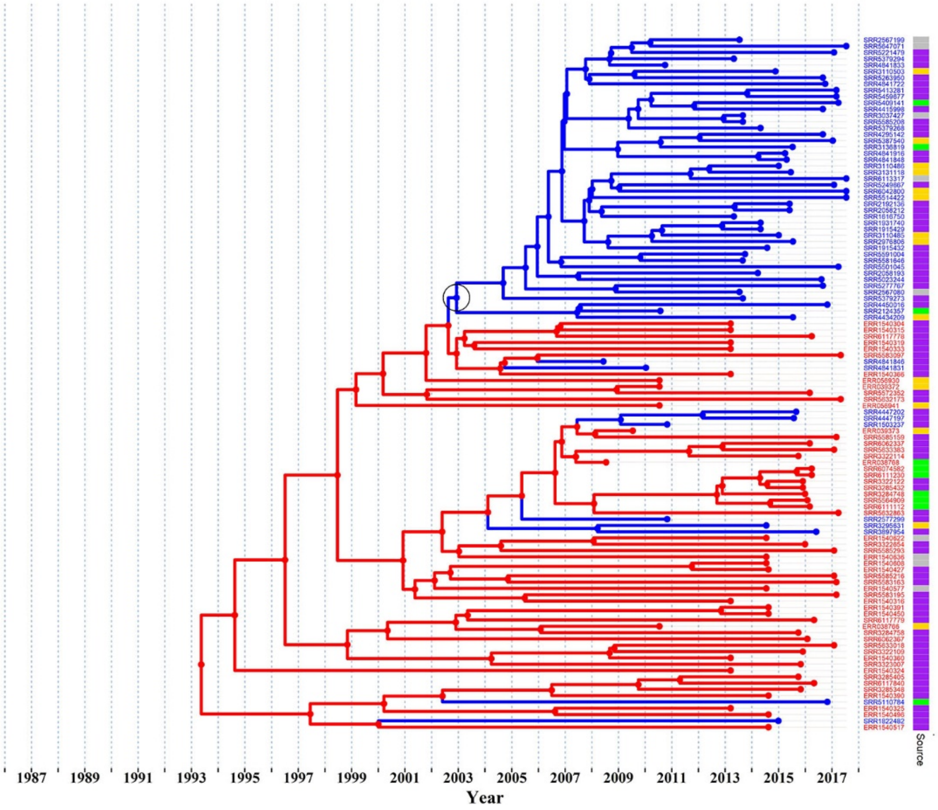
1987
1989
1991
1993
1995
1997
1999
2001
2003
2005
2007
2009
2011
2013
2015
2017
Year
Source

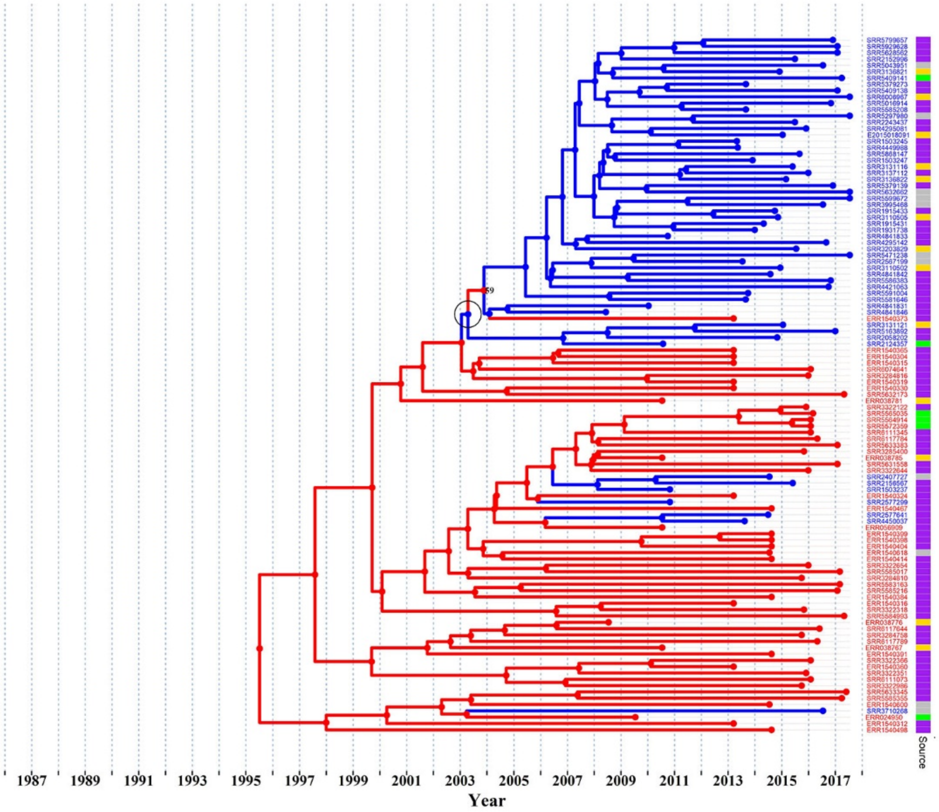
59
1987
1989
1991
1993
1995
1997
1999
2001
2003
2005
2007
2009
2011
2013
2015
2017
Year
Source

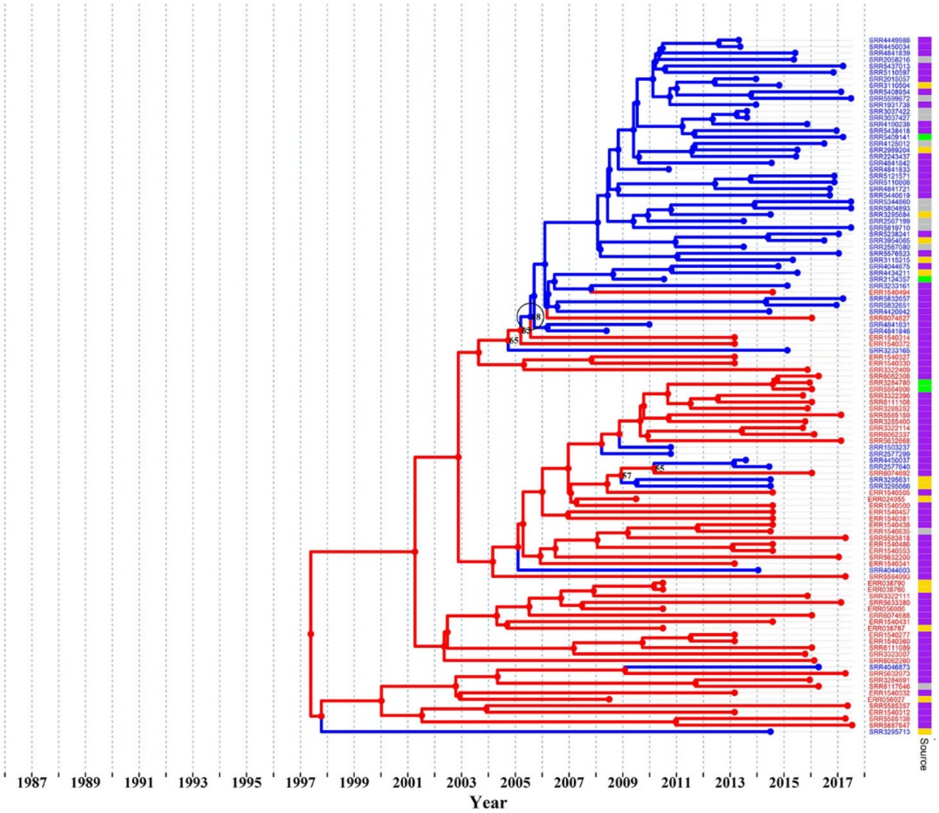
Source
1987
1989
1991
1993
1995
1997
1999
2001
2003
2005
2007
2009
2011
2013
2015
2017
Year

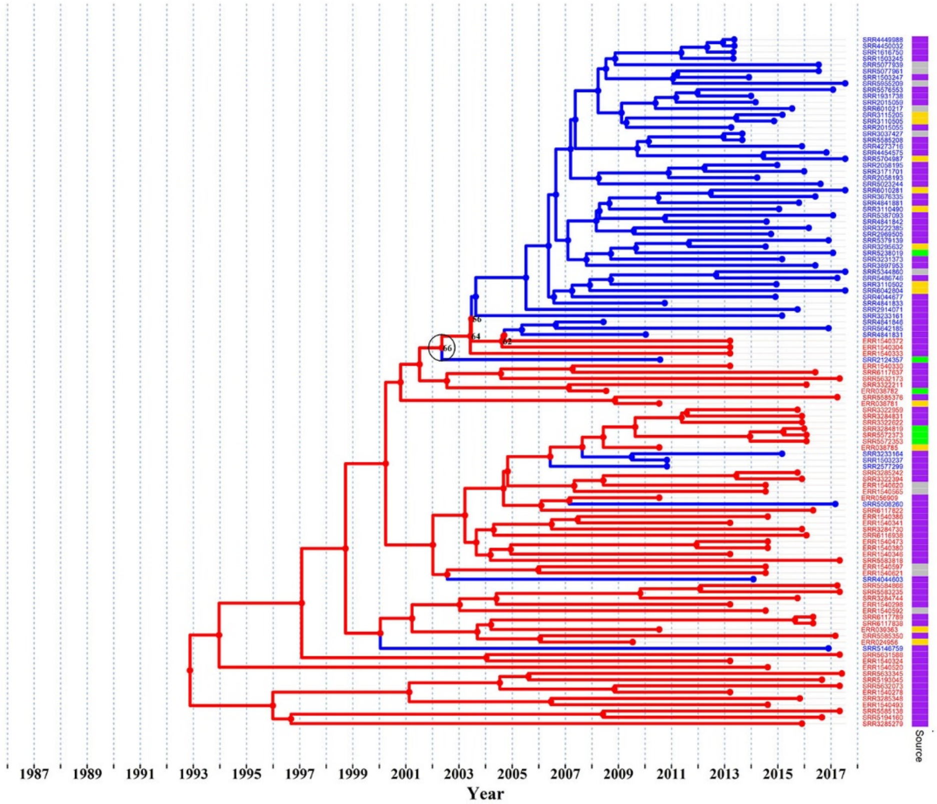
Source
1987
1989
1991
1993
1995
1997
1999
2001
2003
2005
2007
2009
2011
2013
2015
2017
Year

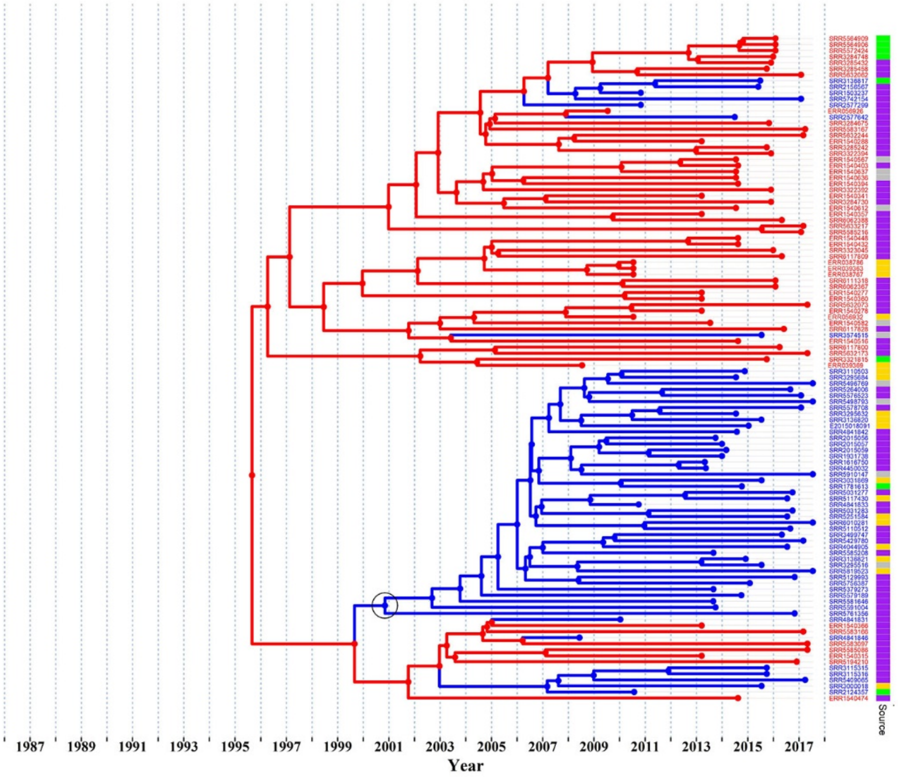
Source
1987
1989
1991
1993
1995
1997
1999
2001
2003
2005
2007
2009
2011
2013
2015
2017
Year

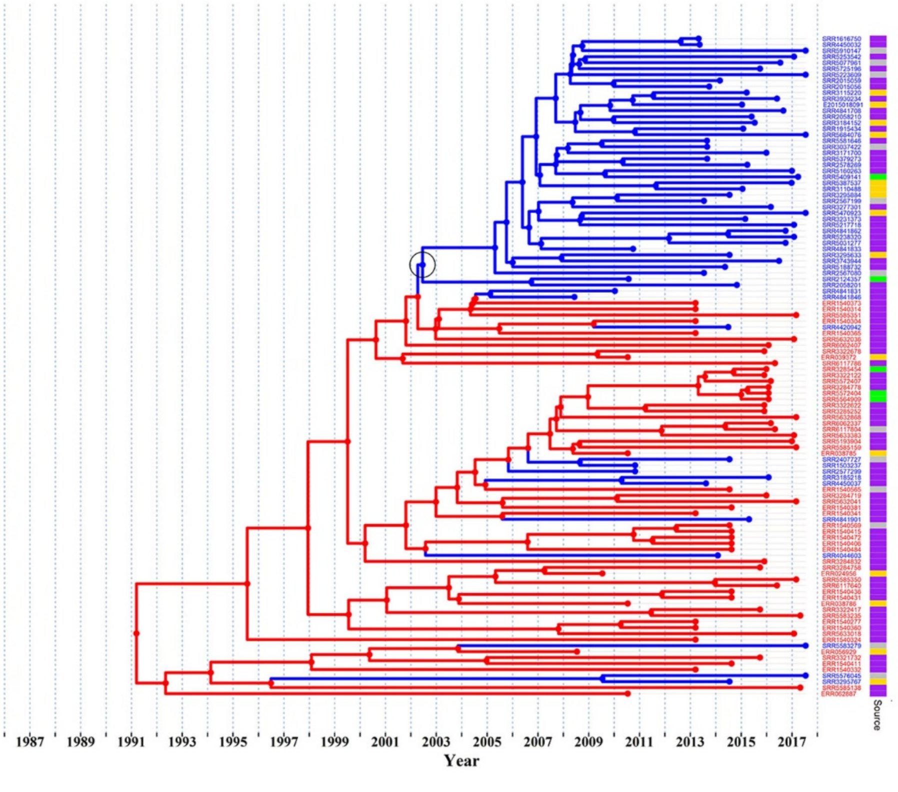
Source
1987
1989
1991
1993
1995
1997
1999
2001
2003
2005
2007
2009
2011
2013
2015
2017
Year

Appendix 2 Figures 1–10. Time scaled phylogenetic analysis of *S.* 4,[5],12:i:- ST34 isolates in subsets 1 to 10 (n ranged between 106 and 110 sequences following duplicates removal). Isolates were collected in USA (blue) and Europe (red) between 2008 and 2017 from multiple sources. Asymmetrical discrete trait analysis model was used to predict the locations on the nodes. The nodes, branches and tree tips were annotated according to the collection location. Nodes with location probabilities below 70% are indicated (with the location probability value). The ancestor node of the main USA *S.* 4,[5],12:i:- ST34 clade is circled (black). In addition, the bacterial isolate source ['Food product' (grey), 'Human' (purple), 'Livestock' (yellow) and 'Other' (green)] is depicted in the heatmap appended to the tree tips.

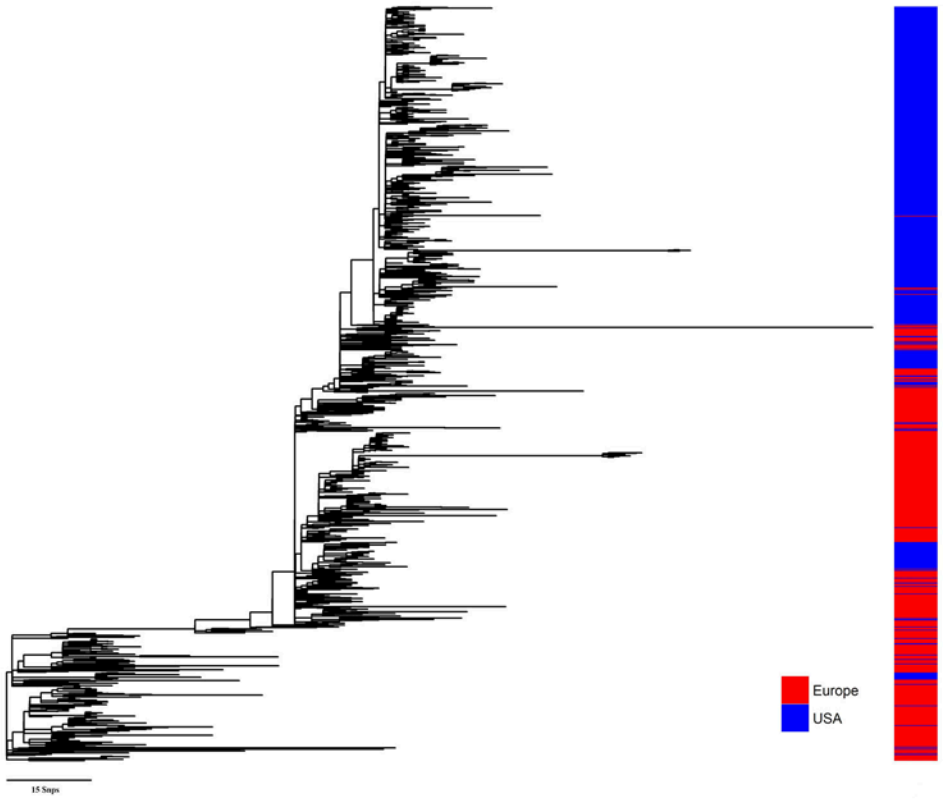

Appendix 2 Figure 11. A maximum likelihood phylogeny tree of the core genome of all *S.* 4,[5],12:i:- ST34 isolates (1431 sequences were included in the analysis, yet after removal of duplicates, 1185 sequences were included in the phylogeny tree; 25,687 variable sites were used for this analysis). Isolates were collected in USA (blue) and Europe (red) between 2008 and 2017 from multiple sources. *Salmonella* Enteritidis isolates (SRR1965760 and SRR3242211) were used as outgroup (not included in the figure).

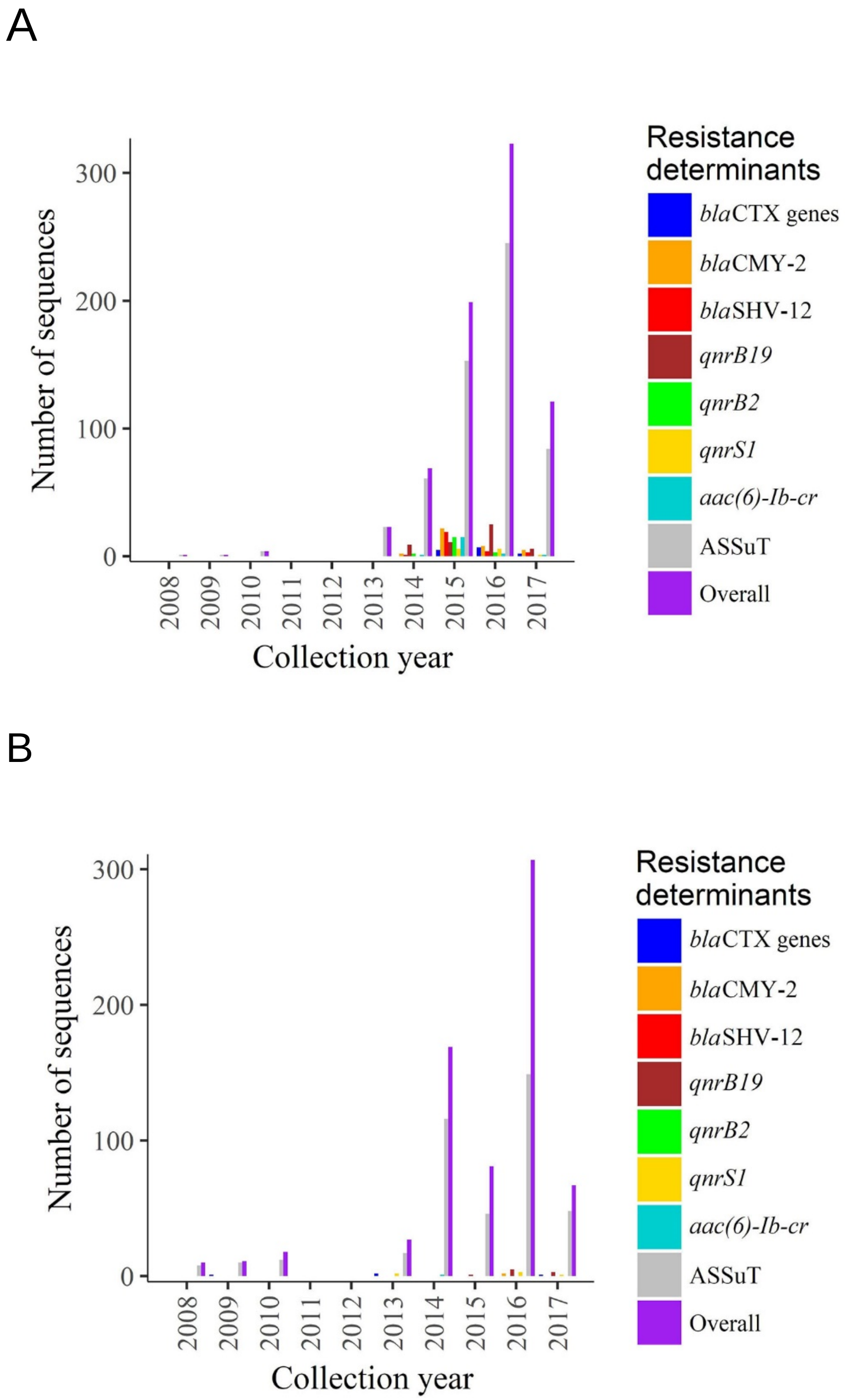

Appendix 2 Figure 12. The number of *S*. 4,[5],12:i:- ST34 sequences at the NCBI repository included in the study population and were collected in the USA (A) and Europe (B) in different years. The graph bars indicate of the overall number (purple) of available sequences and the number of sequences harboring genetic resistance determinants: *bla*$_{\text{CTX-M}}$ genes (blue), *bla*$_{\text{CMY-2}}$ (orange), *bla*$_{\text{SHV-12}}$ (red), *qnrB19* (brown), *qnrB2* (green), *qnrS1* (yellow), *aac(6')-Ib-cr* (turquoise) and ASSuT (grey).

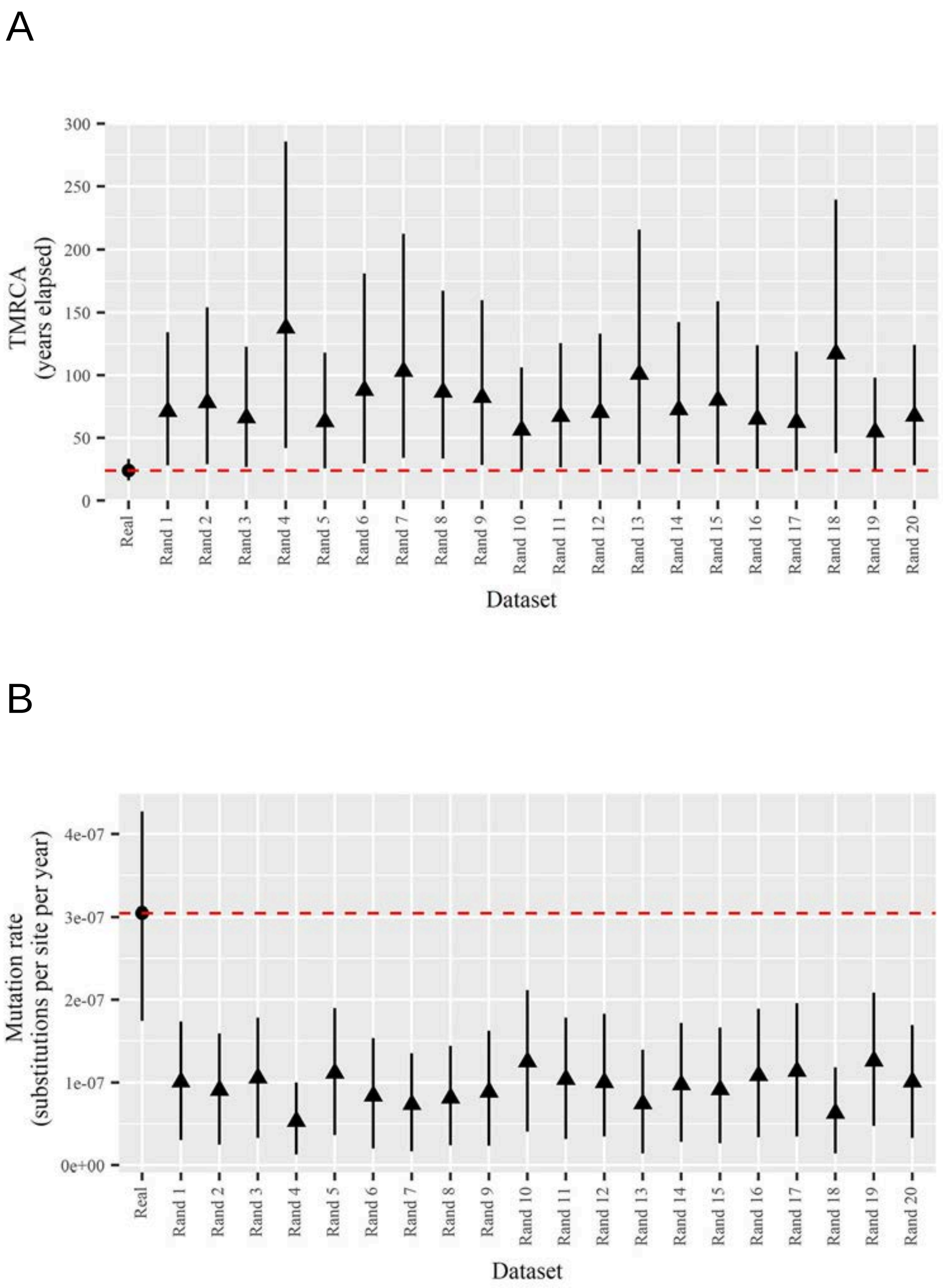

Appendix 2 Figure 13. The mean posterior values [with 95% highest posterior density (HPD) credible interval] of the mutation rate (upper inset) and the time to the most recent common ancestor (TMRCA; lower inset) parameters are indicated for the real data (circle) and the randomized date repeats (triangles). The mean values of the real data are further emphasized with dashed red lines.